Theor Chem Acc (1997) 98:5–15

Theoretical
Chemistry Accounts

Regular Paper

Ab initio self-consistent reaction field calculations on amino acids: asparagine zwitterions in polar medium and gas phase

J.T. López Navarrete, J. Casado, V. Hernández, F.J. Ramírez

Departamento de Química Física, Facultad de Ciencias,Universidad de Málaga, E-29071 Málaga, Spain

Received: 30 December 1996 / Accepted: 17 April 1997

Abstract. A comparative theoretical study of the structure and vibrations of amino acid L-asparagine has been performed on the basis of ab initio Hartree-Fock calculations and the self-consistent reaction field theory. The 3-21G* and 6-31+G* basis sets were used to evaluate quadratic force fields of this amino acid in an aqueous solution and in isolation (gas phase). Previously each of the minimal energy structures was predicted. Geometric parameters, atomic charges, electronic energies, vibrational frequencies, normal mode descriptions and force constants were compared. The results confirmed the 6-31+G* as a suitable basis for the study of polar molecules in polar media.

Key words: Asparagine – Amino acids – Self-consistent reaction field

1 Introduction

Ab initio calculations are being performed extensively to study the structure and vibrations of medium-size molecules, like amino acids and small peptides. Most of the currently available force fields for these molecules involve isolated species. It is known that the environment has a critical effect on amino acids [1–5], whose structure changes from neutral to zwitterionic on changing from isolation to a polar medium. As the natural environment for biological molecules such as amino acids is the aqueous solution, it is of interest to provide force fields and structural data of zwitterionic amino acids from ab initio methodologies.

In this paper we present the results of an ab initio study of the amino acid L-asparagine, $H_3N^+—CH(CO_2^-)—CH_2—CONH_2$, (Fig. 1). The vibrational spectra of this molecule in solid state [6] and in solution [7] have recently been reported and assigned on the basis of isotopic labelling and semiempirical calculations [8]. Here we report a comparative study of the structure and vibrational spectrum of asparagine involving two basis sets, 3-21G* and 6-31+G*, and two different environments, in a vacuum and in an aqueous polar medium. Recent advances in quantum-chemical calculations have led us to investigate biological systems using more realistic theoretical models. In the present paper the solvent effects have been simulated using a self-consistent reaction field (SCRF) model [9–11].

Correspondence to: F.J. Ramírez

2 Computational method

The equilibrium geometries of the asparagine molecule were predicted by restricted Hartree-Fock (RHF) theory using the 3-21G* and 6-31+G* basis sets [12]. We employed the GAUSSIAN-92 program [13] to generate both gas phase (isolated) and SCRF optimized structures of this amino acid as a zwitterion. The isolated structures were characterized in a local, non-absolute minimum of the potential energy surface, and by using the optimized solvated structures as the starting points of the minimization processes in both cases. The spherical cavity formalism was applied in the SCRF calculations. The cavity radius was adjusted from the molecular density, as reported elsewhere [7, 9], at 3.74 Å. The final structures were always obtained, allowing all the geometric parameters to vary independently until reaching the convergence criteria.

Cartesian force constants were each evaluated within the same theoretical scheme used for the geometry optimizations. Second derivatives of the molecular energy were computed analytically. All the ab initio calculations were performed on a Convex 240 at the CICA Computer Center in Seville (Spain). Maximal forces (in atomic units) after geometry optimization were lower than $3.7.10^{-4}$. Maximal deviations from ideally zero translation and rotation frequencies were lower than 3.8 cm^{-1}. Frequencies were obtained by diagonalization of a mass-weighted cartesian force constant matrix. Infrared absorption intensities were evaluated from atomic polar tensors [14]. The cartesian force constants were transformed into a set of non-redundant locally symmetrized internal coordinates, defined according to Pulay

methodology [15]. This step allows a more useful description of the vibrational potential energy and makes further calculations easier. The force field in internal coordinates was subsequently scaled to compensate for systematic overestimations. Frequencies and normal coordinates were calculated by the Wilson FG matrix method [16].

3 Results and discussion

We have listed in Tables 1–3 the results on bond distances and angles for the optimized structures of the asparagine molecule. The four structures are depictured in Fig. 2. Table 4 shows the electronic energies and dipole moments, while Table 5 lists the Mulliken charge

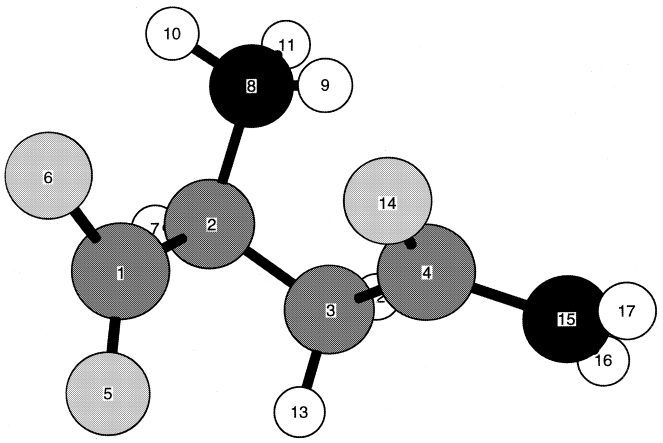

Fig. 1. Atomic numbering used in this work for zwitterionic asparagine

Table 1. Bond lengths (Å) obtained for the optimized structures of asparagine

Bond[a]	3-21G* gas phase	3-21G* SCRF	6-31+G* gas phase	6-31+G* SCRF	Exp.[b]
C_1—C_2	1.585	1.579	1.571	1.564	1.518
C_1—O_5	1.232	1.239	1.218	1.227	1.247
C_1—O_6	1.257	1.254	1.233	1.241	1.265
C_2—C_3	1.529	1.529	1.526	1.530	1.511
C_2—H_7	1.079	1.079	1.082	1.083	0.973
C_2—N_8	1.523	1.525	1.503	1.501	1.501
C_3—C_4	1.516	1.514	1.516	1.523	1.516
C_3—H_{12}	1.077	1.076	1.079	1.083	1.006
C_3—H_{13}	1.081	1.082	1.085	1.086	0.987
C_4—O_{14}	1.237	1.233	1.214	1.217	1.243
C_4—N_{15}	1.331	1.339	1.339	1.332	1.332
N_8—H_9	1.027	1.030	1.016	1.015	0.954
N_8—H_{10}	1.074	1.047	1.026	1.010	0.932
N_8—H_{11}	1.008	1.011	1.005	1.011	0.935
N_{15}—H_{16}	1.003	1.000	0.998	0.998	0.929
N_{15}—H_{17}	0.999	0.998	0.998	0.999	0.919
O_6···H_{10}	1.60	1.72	1.83	2.10	–
O_{14}···H_9	1.90	1.87	1.98	1.99	–

[a] See Fig. 1 for numbering
[b] Data from Ref. [22]

Table 2. Bond angles (in degrees) obtained for the optimized structures of asparagine

Angle[a]	3-21G* gas pahse	3-21G* SCRF	6-31+G* gas phase	6-31+G* SCRF	Exp.[b]
$C_2C_1O_5$	115.3	115.4	114.2	116.2	118.2
$C_2C_1O_6$	111.6	113.0	112.8	114.1	115.7
$C_1C_2C_3$	109.3	109.9	113.6	118.7	115.7
$C_1C_2H_7$	110.6	110.6	107.9	105.5	104.4
$C_1C_2N_8$	113.0	104.2	105.8	107.5	110.8
$C_3C_2H_7$	112.1	111.7	109.9	107.8	110.9
$H_7C_2N_8$	109.0	108.5	107.0	105.7	103.1
$C_2C_3C_4$	107.4	107.4	110.1	113.7	112.5
$C_2C_3H_{12}$	106.6	107.2	107.1	107.4	105.3
$C_2C_3H_{13}$	111.8	111.6	111.2	110.1	106.7
$C_4C_3H_{12}$	112.0	111.9	112.2	108.5	109.2
$C_4C_3H_{13}$	108.3	108.9	107.3	109.6	108.3
$C_3C_4O_{14}$	119.1	119.8	119.1	120.1	120.5
$C_3C_4N_{15}$	116.0	115.9	117.3	116.4	116.5
$O_{14}C_4N_{15}$	124.6	123.9	123.4	123.3	122.9
$C_2N_8H_9$	108.9	108.3	110.0	108.2	109.5
$C_2N_8H_{10}$	97.3	99.9	102.9	107.6	109.2
$C_2N_8H_{11}$	114.6	114.3	114.3	113.8	112.2
$H_9N_8H_{10}$	110.9	110.1	108.9	107.2	109.5
$H_9N_8H_{11}$	111.0	110.4	109.0	108.9	112.1
$H_{10}N_8H_{11}$	113.2	113.1	111.3	110.5	104.1
$C_4N_{15}H_{16}$	118.6	119.4	118.3	122.1	119.8
$C_4N_{15}H_{17}$	118.2	118.9	116.6	118.4	122.1
$H_{16}N_{15}H_{17}$	119.4	118.7	116.4	115.9	117.2
$O_6H_{10}N_8$	141.7	141.3	137.7	129.9	–
$O_{14}H_9N_8$	131.6	126.8	120.7	106.9	–

[a] See Figure 1 for numbering
[b] Data from Ref. [22]

Table 3. Dihedral angles (in degrees) obtained for the optimized structures of asparagine

Dihedral angle[a]	3-21G* gas phase	3-21G* SCRF	6-31+G* gas phase	6-31+G* SCRF	Exp.[b]
$O_5C_1C_2C_3$	−40.37	−40.69	−36.48	−37.19	−47.5
$O_5C_1C_2H_7$	83.57	83.32	85.80	83.80	74.7
$O_5C_1C_2N_8$	−159.88	−160.24	−159.85	−163.60	−174.9
$O_6C_1C_2C_3$	137.83	136.61	143.81	147.71	136.6
$O_6C_1C_2H_7$	−98.23	−99.39	−93.91	−91.29	−101.2
$O_6C_1C_2N_8$	18.31	17.06	20.44	21.30	9.2
$C_1C_2C_3C_4$	−59.49	−62.53	−61.89	−77.81	−53.8
$C_1C_2C_3H_{12}$	61.00	57.74	60.45	42.32	65.1
$C_1C_2C_3H_{13}$	−178.48	178.71	179.21	158.63	−172.4
$C_1C_2N_8H_9$	98.71	101.59	95.05	77.63	81.6
$C_1C_2N_8H_{10}$	−16.49	−13.50	−20.92	−38.05	−38.4
$C_1C_2N_8H_{11}$	−137.59	133.93	−141.82	−161.01	−153.2
$C_2C_3C_4O_{14}$	−72.00	−76.96	−68.79	14.91	3.1
$C_2C_3C_4N_{15}$	102.69	97.41	110.82	−165.42	−177.0
$H_{12}C_3C_4O_{14}$	170.55	166.22	171.88	−104.78	−113.5
$H_{12}C_3C_4N_{15}$	−14.75	−19.41	−8.50	−75.09	66.4
$H_{13}C_3C_4O_{14}$	48.88	44.02	52.47	138.75	120.7
$H_{13}C_3C_4N_{15}$	−136.43	−141.61	−127.91	−41.58	−59.3
$C_3C_4N_{15}H_{16}$	−18.67	−14.75	−23.10	12.55	4.3
$C_3C_4N_{15}H_{17}$	−176.80	−175.33	−170.01	170.90	173.0
$O_{14}C_4N_{15}H_{16}$	155.78	159.27	156.50	−167.79	−175.8
$O_{14}C_4N_{15}H_{17}$	−2.35	−1.30	9.59	−9.44	−7.1
$N_8H_9O_{14}C_4$	1.2	5.9	−8.7	40.0	–
$N_8H_{10}O_6C_1$	−3.5	−1.7	−4.2	−20.7	–

[a] See Fig. 1 for numbering
[b] Data from Ref. [22]

distributions. As can be seen in Fig. 2, only the 6-31+G* basis set allows the molecule to adopt a more elongated conformation in order that it can be better solvated. This conclusion is in good agreement with the previous work of several authors [9, 17] on theoretical calculations concerning dipolar species in solution, as zwitterions and related molecules. Thus, the longest interatomic distance ranges from 5.36 Å (gas phase) to 5.45 Å (solution) for 3-21G*, and from 5.49 Å (gas phase) to 6.09 Å (solution) for 6-31+G*.

Data from Table 4 also are in agreement with this fact. The solvent environment decreases the electronic

Table 4. Total energies (in hartrees), relative energies (in kcal·mol^{-1}) and dipole moments (in debye) for the optimized structures of asparagine in the zwitterionic form

	3-21G* gas phase	3-21G* SCRF	6-31+G* gasphase	6-31+G* SCRF
Total energy	−486.90413	−486.28458	−489.64290	−489.73979
Relative energy[a]	0.0	−15.27	0.0	−60.30
Dipole moment	6.0207	8.0348	7.3307	17.2127

[a] Energies relatives to the gas phase structure in each case

Table 5. Atomic charges calculated for the asparagine molecule

Atom[a]	3-21G* gas phase	3-21G* SCRF	6-31+G* gas phase	6-31+G* SCRF
C_1	0.934	0.913	0.527	0.598
C_2	−0.229	−0.226	0.217	0.084
C_3	−0.512	−0.514	−0.590	−0.561
C_4	0.858	0.864	0.679	0.722
O_5	−0.715	−0.745	−0.682	−0.733
O_6	−0.736	−0.749	−0.719	−0.789
H_7	0.286	0.301	0.248	0.257
N_8	−0.906	−0.896	−1.153	−1.127
H_9	0.434	0.449	0.562	0.574
H_{10}	0.465	0.450	0.566	0.528
H_{11}	0.390	0.413	0.474	0.526
H_{12}	0.291	0.280	0.273	0.291
H_{13}	0.260	0.296	0.238	0.276
O_{14}	−0.671	−0.654	−0.646	−0.672
N_{15}	−0.921	−0.921	−0.907	−0.927
H_{16}	0.404	0.387	0.469	0.472
H_{17}	0.368	0.352	0.444	0.482
CO_2^-	−0.517	−0.581	−0.874	−0.924
NH_3^+	0.383	0.416	0.449	0.501

[a] See Fig. 1 for numbering

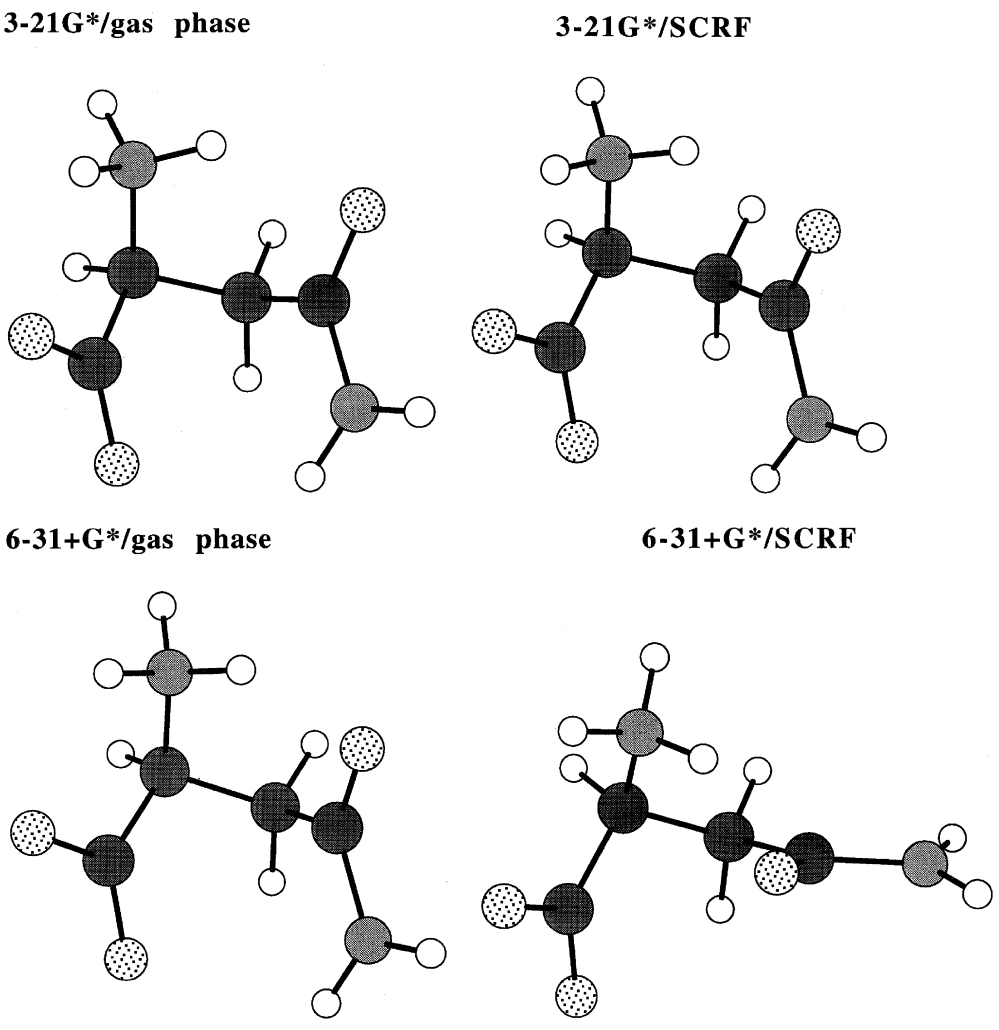

Fig. 2. Optimized structures predicted for asparagine by ab initio methods

energy of the asparagine molecule by 15.27 kcal/mol for the 3-21G* basis set and by 60.30 kcal/mol for the 6-31+G* one. The last value agrees with the solvation energies reported for several conformations of zwitterionic glycine using the 4-31G basis set [4]. The dipole moment obtained for gas-phase zwitterionic asparagine using the 6-31+G* basis set, 7.33 D, is consistent with those reported for other amino acids of similar size, such as cysteine (8.66 D), serine (8.43 D) or threonine (8.84 D), from ab initio 6-31G** calculations [18]. In previous work using the 6-31G basis set [2] the dipole moments for the aforementioned amino acids were calculated appreciably higher, namely, 12.47, 12.91 and 12.78 D. These data clearly indicate the convenience of using polarization functions in ab initio calculations on this type of molecules. For asparagine, the data listed in Table 4 show a critical enhancement of the dipole moment of the zwitterionic asparagine molecule, on changing from an isolated to a solvated state, particularly when the highest level basis set is used. This behaviour obviously results from the fact that the solvated molecule is elongated with respect to the isolated molecule, and that the calculated atomic charges, listed in Table 5, show modifications in the solute charge distribution induced by the reaction field as a result of the environment, in accordance with the Onsager model [19]. In a series of recently reported papers focusing on the study of amino acid side chains [20, 21] this trend was undoubtedly confirmed. In our case significant intramolecular charge fluxes to the strongly polar end

Table 6. Symmetrized Pulay coordinates used in this work for the vibrational analysis of the asparagine molecule

Number[a]	Coordinate[b]	Symbol	Description
1	$r_{1\ 2}$	ν(CC)	C—C stretch
2	$r_{2\ 3}$	ν(CC)	C—C stretch
3	$r_{3\ 4}$	ν(CC)	C—C stretch
4	$2^{-1/2}(r_{3\ 12} + r_{3\ 13})$	$\nu_s(CH_2)$	CH_2 sym. stretch
5	$2^{-1/2}(r_{3\ 12} - r_{3\ 13})$	$\nu_a(CH_2)$	CH_2 antisym. stretch
6	$r_{4\ 14}$	ν(C=O)	C=O stretch
7	$r_{4\ 15}$	$\nu(C—NH_2)$	$C—NH_2$ stretch
8	$r_{2\ 7}$	ν(CH)	C—H stretch
9	$r_{2\ 8}$	$\nu(C—NH_3^+)$	$C—NH_3^+$ stretch
10	$r_{1\ 5}$	$\nu(C—O_5)$	CO_2^- stretch
11	$r_{1\ 6}$	$\nu(C—O_6)$	CO_2^- stretch
12	$r_{8\ 9}$	$\nu(N—H_9)$	NH_3^+ stretch
13	$r_{8\ 10}$	$\nu(N—H_{10})$	NH_3^+ stretch
14	$r_{8\ 11}$	$\nu(N—H_{11})$	NH_3^+ stretch
15	$2^{-1/2}(r_{15\ 16} + r_{15\ 17})$	$\nu_s(NH_2)$	NH_2 sym. stretch
16	$2^{-1/2}(r_{15\ 16} - r_{15\ 17})$	$\nu_a(NH_2)$	NH_2 antisym. stretch
17	$26^{-1/2}(5\beta_{12\ 3\ 4} + \beta_{2\ 3\ 4})$	$\delta(CH_2)$	CH_2 scissor
18	$26^{-1/2}(5\beta_{2\ 3\ 4} + \beta_{12\ 3\ 13})$	δ(skel)	CCC bend
19	$1/2(\beta_{12\ 3\ 4} - \beta_{13\ 3\ 4} + \beta_{2\ 3\ 12} - \beta_{2\ 3\ 13})$	$r(CH_2)$	CH_2 rock
20	$1/2(\beta_{12\ 3\ 4} + \beta_{13\ 3\ 4} - \beta_{2\ 3\ 12} - \beta_{2\ 3\ 13})$	$\omega(CH_2)$	CH_2 wagg
21	$1/2(\beta_{12\ 3\ 4} - \beta_{13\ 3\ 4} - \beta_{2\ 3\ 12} + \beta_{2\ 3\ 13})$	$t(CH_2)$	CH_2 twist
22	$6^{-1/2}(2\beta_{5\ 1\ 6} - \beta_{5\ 1\ 2} - \beta_{6\ 1\ 2})$	$\delta(CO_2^-)$	CO_2^- in-pl. bend
23	$2^{-1/2}(\beta_{5\ 1\ 2} - \beta_{6\ 1\ 2})$	$\delta(CO_2^-)$	CO_2^- in-pl. bend
24	ϕ_1	$\gamma(OCO^-)$	OCO^- out-pl. bend
25	$6^{-1/2}(\beta_{11\ 8\ 10} + \beta_{10\ 8\ 9} + \beta_{9\ 8\ 11} - \beta_{2\ 8\ 9} - \beta_{2\ 8\ 10} - \beta_{2\ 8\ 11})$	$\delta_s(NH_3^+)$	NH_3^+ sym. bend
26	$6^{-1/2}(2\beta_{11\ 8\ 10} - \beta_{10\ 8\ 9} - \beta_{9\ 8\ 11})$	$\delta_a(NH_3^+)$	NH_3^+ antisym. bend
27	$2^{-1/2}(\beta_{10\ 8\ 9} - \beta_{9\ 8\ 11})$	$\delta_a(NH_3^+)$	NH_3^+ antisym. bend
28	$6^{-1/2}(2\beta_{2\ 8\ 9} - \beta_{2\ 8\ 10} - \beta_{2\ 8\ 11})$	$r(NH_3^+)$	NH_3^+ rock
29	$2^{-1/2}(\beta_{2\ 8\ 10} - \beta_{2\ 8\ 11})$	$r(NH_3^+)$	NH_3^+ rock
30	$6^{-1/2}(\beta_{1\ 2\ 7} - \beta_{8\ 2\ 7} - \beta_{3\ 2\ 7})$	δ(CH)	C—H bend
31	$2^{-1/2}(\beta_{8\ 2\ 7} + \beta_{3\ 2\ 7})$	δ(CH)	C—H bend
32	$18^{-1/2}(4\beta_{1\ 2\ 8} + \beta_{1\ 2\ 3} + \beta_{3\ 2\ 8})$	δ(skel)	CCN bend
33	$18^{-1/2}(4\beta_{3\ 2\ 8} + \beta_{1\ 2\ 3} + \beta_{1\ 2\ 8})$	δ(skel)	CCN bend
34	$18^{-1/2}(4\beta_{1\ 2\ 3} + \beta_{1\ 2\ 8} + \beta_{3\ 2\ 8})$	δ(skel)	CCC bend
35	$6^{-1/2}(2\beta_{16\ 15\ 17} - \beta_{4\ 15\ 17} - \beta_{4\ 15\ 16})$	$\gamma(NH_2)$	NH_2 bend
36	$2^{-1/2}(\beta_{4\ 15\ 17} - \beta_{4\ 15\ 16})$	$\gamma(NH_2)$	NH_2 rock
37	ϕ_{15}	$r(NH_2)$	NH_2 out-pl. bend
38	$6^{-1/2}(2\beta_{3\ 4\ 14} - \beta_{14\ 4\ 15} - \beta_{3\ 4\ 15})$	$\delta(CONH_2)$	$CONH_2$ in-pl. bend
39	$2^{-1/2}(\beta_{14\ 4\ 15} - \beta_{3\ 4\ 15})$	$\delta(CONH_2)$	$CONH_2$ in-pl. bend
40	ϕ_{14}	γ(NCO)	NCO out-pl. bend
41	$\tau_{4\ 15}$	$\tau(NH_2)$	NH_2 torsion
42	$\tau_{1\ 2}$	$\tau(CO_2^-)$	CO_2^- torsion
43	$\tau_{2\ 8}$	$\tau(NH_3^+)$	NH_3^+ torsion
44	$\tau_{2\ 3}$	τ(CC)	CC torsion
45	$\tau_{3\ 4}$	τ(CC)	CC torsion

[a] Arbitrary numbering
[b] The atomic numbering is defined in Fig. 1
$r_{i\ j}$ = stretching vibrations of the bond between atoms i and j
$\beta_{i\ j\ k}$ = in-plane bending vibration of the angle between atoms i, j and k
ϕ_i = out-of-plane bending vibration of atom i
$\tau_{i\ j}$ = torsion vibration with respect to the bond between atoms i and j, which were defined as described in Refs. 27 and 28

groups, ammonium and carboxylate, were observed, thus enhancing the zwitterionic character of this amino acid in aqueous solution. As expected, this enhancement is greater when the 6-31+G* basis set is used, and is in good agreement with dipole moment results. In this way, the calculated charges for the carboxylate moiety show the difficulties we have in characterizing dipolar species in solution without using ab initio basis sets that are large enough; as a significant example, data from Table 5 show that the gas phase asparagine 6-31+G* charge distribution is closer to a zwitterionic structure than that obtained by 3-21G* for the solvated molecule.

Concerning the optimized geometrical parameters, (Tables 1–3), only data for monohydrated asparagine are available, from X-ray diffraction techniques [22], and these are included in the aforementioned tables. In addition to the solute-solvent effects, we could expect two intramolecular interactions involving the NH_3^+ group and in turn the CO_2^- and the C=O (amide) groups. As we will discuss later, two non-bonded H···O distances are within the hydrogen bond range [23]. However, in some cases the related N—H···O angles are so far from linearity that they can be better classified as short van der Waals intramolecular contacts than as weak hydrogen bonds. Regarding the calculated optimized conformations we deduce the presence of a moderate hydrogen bond $O_{14}\cdots H_9$ in the four structures depicted in Fig. 2, the lengths of which range from 1.87 to 1.99 Å. A different behaviour is observed for the interaction involving the O_6 and H_{10} atoms; whereas a strong interatomic contact (1.60 Å) exists in the 3-21G* structure of the gas phase molecule, it relaxes slightly in

Table 7. 3-21G*/gas phase and experimental frequencies[a] cm^{-1}) and infrared intensities ($km \cdot mol^{-1}$) calculated for asparagine

Vibration[b]	Calc.	Exp.[c]	IR int.	P. E. D. (greater than 10%)[d]
ν_1	3463		96.15	$95\nu_a(NH_2)$
ν_2	3343		100.88	$94\nu_s(NH_2)$
ν_3	3336		103.78	$98\nu(N—H_{11})$
ν_4	3056		239.90	$98\nu(N—H_9)$
ν_5	3014	2965	0.48	$84\nu_a(CH_2) + 15\nu_s(CH_2)$
ν_6	2971	2945	8.31	$98\nu(CH)$
ν_7	2939	2907	8.70	$84\nu_s(CH_2) + 16\nu_a(CH_2)$
ν_8	2473		426.49	$98\nu(N—H_{10})$
ν_9	1733		172.07	$54\nu(C—O_5) + 34\nu(C—O_6)$
ν_{10}	1684		30.18	$56\delta_a(NH_3^+) + 22\nu((C=O)$
ν_{11}	1662		288.78	$50\delta_a(NH_3^+) + 20\delta(NH_2) + 15\nu(C=O)$
ν_{12}	1648	1611	52.04	$70\delta(NH_2) + 17\delta_a(NH_3^+)$
ν_{13}	1594	1538	273.79	$43\delta_a(NH_3^+) + 32\nu(C=O) + 18\delta_s(NH_3^+)$
ν_{14}	1474		37.81	$100\delta(CH_2)$
ν_{15}	1422	1450	550.78	$56\delta_s(NH_3^+) + 24\delta_a(NH_3^+) + 13\nu(C—O_5) + 12\delta(NH_2)$
ν_{16}	1385	1421	220.29	$28\nu(C—NH_3^+) + 17\nu(CC) + 13\delta(CONH_2) + 12\delta(CH)$
ν_{17}	1338	1404	36.25	$58\omega(CH_2) + 14\delta(CH)$
ν_{18}	1320	1356	78.21	$55\delta(CH) + 22r(NH_3^+)$
ν_{19}	1291	1329	79.52	$28r(NH_3^+) + 27t(CH_2) + 16\delta(CH) + 11\nu(CC)$
ν_{20}	1242	1314	208.12	$54\nu(C—O_6) + 21\nu(C—O_5) + 20\delta(CO_2^-) + 12\nu(CC)$
ν_{21}	1197	1227	34.74	$31\delta(CH) + 30t(CH_2) + 11r(NH_2) + 10\nu(CC)$
ν_{22}	1153	1151	23.60	$33\delta(CH) + 32r(NH_3^+) + 11\nu(C=O)$
ν_{23}	1120	1120	4.64	$36r(NH_2) + 18t(CH_2) + 17\nu(C—NH_2)$
ν_{24}	1097		59.80	$80r(NH_3^+) + 32\delta(CH) + 17\delta(skel)$
ν_{25}	1003	983	8.51	$33\nu(CC) + 30r(CH_2) + 28\nu(C—NH_3^+) + 15\delta(skel)$
ν_{26}	977	926	17.27	$59r(CH_2) + 31\nu(CC)$
ν_{27}	884	864	55.05	$80\delta(skel) + 20\nu(CC) + 16r(NH_3^+) + 13\gamma(NCO)$
ν_{28}	817	827	27.94	$53\nu(C—NH_3^+) + 18\nu(CC) + 18\gamma(NCO) + 10r(CH_2)$
ν_{29}	805	800	268.43	$29\nu(CC) + 26\delta(CO_2^-) + 15\gamma(NCO) + 15\delta(skel)$
ν_{30}	763	765	66.93	$50\nu(CC) + 10\gamma(OCO^-)$
ν_{31}	758		47.26	$41\delta(CO_2^-) + 20\gamma(OCO^-) + 14\nu(C—NH_3^+)$
ν_{32}	686		56.78	$50\gamma(NH_2) + 16\gamma(NCO) + 11\nu(CC)$
ν_{33}	636	605	23.95	$86\tau(NH_2)$
ν_{34}	570		3.35	$33\nu(CC) + 27\delta(skel) + 22\delta(CO_2^-) + 22\gamma(OCO^-)$
ν_{35}	529		18.44	$60\delta(CONH_2) + 12\nu(CC) + 10\tau(NH_2)$
ν_{36}	510	520	29.13	$38\delta(CO_2^-) + 26\nu(CC) + 14\delta(skel)$
ν_{37}	472		2.68	$114\tau(NH_3^+)$
ν_{38}	446		10.56	$62\delta(CONH_2) + 54\tau(skel) + 28r(CH_2)$
ν_{39}	418		6.67	$110\delta(skel) + 11\delta(CO_2^-)$
ν_{40}	341		80.10	$64\delta(skel) + 39\delta(CO_2^-) + 38\nu(N—H_{10}) + 12r(NH_3^+)$
ν_{41}	269		26.88	$58\delta(skel) + 12\delta(CO_2^-) + 11\gamma(NCO)$
ν_{42}	206		21.55	$44\tau(skel) + 35\delta(skel) + 19\tau(CO_2^-) + 14\nu(N—H_{10})$
ν_{43}	150		43.53	$78\tau(skel) + 13\tau(NH_3^+) + 11\tau(CO_2^-)$
ν_{44}	101		9.01	$103\tau(CO_2^-) + 64\tau(skel) + 40\delta(skel)$
ν_{45}	84		12.29	$90\tau(skel) + 82\tau(CO_2^-) + 60\tau(NH_3^+)$

[a] Scaled by 0.9
[b] Arbitrary numbering
[c] Data from Ref. 7
[d] See Table 6 for coordinate descriptions. Contributions from coordinates with the same character have been added to clarify the normal mode descriptions

the 3-21G*/SCRF and 6-31+G* structures (1.72 and 1.83 Å, respectively) and almost disappears in the 6-31+G*/SCRF structure (2.10 Å). These interatomic distances are listed in Table 6, which also includes the N—H···O angles and N—H···O—C dihedrals. It is interesting to observe that these angles correlate quite well with the related distances in that the shortest O···H contact corresponds to the longest N—H···O angle in both intramolecular interactions. In the same way, only the 6-31+G*/SCRF structure deviates significantly from the N—H···O—C planarity (20.7 and 40.0 deg.), while the rest of the optimized structures deviate by less than 10 deg., especially those calculated by the 3-21G* basis set. The reason for this behaviour can be found in the solute-solvent interactions. Figure 2 shows that the conformation of the amide group changes to allow for a more intense electrostatic interaction between amide-hydrogen atoms and solvent molecules. As a consequence of this change, the NH_3^+ moiety turns to safeguard the $O_{14}\cdots H_9$ hydrogen bond, so that the $O_6\cdots H_{10}$ interaction is simultaneously broken.

In relation to the optimized geometries, the best agreement with the experimental data corresponds, as expected, to the 6-31+G* values. In previous papers [24–26] this fact has been used by several authors to study the vibrational properties of molecules in the solid state from force fields of the same molecules in a simulated aqueous environment, the lowest energy structure corresponding to the zwitterion in both cases. Concerning the bond lengths, Table 1 shows that the optimized values are more basis set dependent than solvent dependent in this case. Two bond lengths monotonically

Table 8. 3-21G*/SCRF and experimental frequencies[a] (cm^{-1}) and infrared intensities ($km \cdot mol^{-1}$) calculated for asparagine

Vibration[b]	Calc.	Exp.[c]	IR int.	P.E.D. (greater than 10%)[d]
ν_1	3481		100.16	$99\nu_a(NH_2)$
ν_2	3363		100.53	$99\nu_s(NH_2)$
ν_3	3306		180.77	$99\nu(N—H_{11})$
ν_4	3018	2965	18.23	$79\nu(CH_2 + 16\nu_s(CH_2)$
ν_5	3014		338.16	$94\nu(N—H_9)$
ν_6	2970	2945	13.48	$97\nu(CH)$
ν_7	2939	2907	1.92	$81\nu_s(CH_2) + 18\nu_a(CH_2)$
ν_8	2805		382.08	$94\nu(N—H_{10})$
ν_9	1702		231.60	$43\nu(C—O_5) + 32\nu(C—O_6)$
ν_{10}	1689		28.31	$70\delta_a(NH_3^+) + 17\nu((C=O)$
ν_{11}	1670		182.27	$49\delta_a(NH_3^+) + 27\nu(C=O)$
ν_{12}	1642	1611	128.78	$90\delta(NH_2)$
ν_{13}	1593	1538	233.40	$51\delta_a(NH_3^+) + 30\nu(C=O) + 11\delta_a(NH_3^+)$
ν_{14}	1475		181.05	$85\delta(CH_2) + 18\delta_s(NH_3^+)$
ν_{15}	1460	1450	800.96	$57\delta_s(NH_3^+) + 19\delta(CH_2) + 12\delta_a(NH_3^+) + 10\nu(C—O_5)$
ν_{16}	1381	1421	205.52	$21\omega(CH_2) + 20\delta(CH) + 16\nu(CC)$
ν_{17}	1341	1404	68.27	$47\omega(CH_2) + 13\delta(CH) + 11t(CH_2)$
ν_{18}	1324	1356	122.68	$55\delta(CH) + 15r(NH_3^+)$
ν_{19}	1295	1329	56.21	$26r(NH_3^+) + 17t(CH_2) + 17\nu(CC) + 15\delta(CH)$
ν_{20}	1262	1314	289.78	$49\nu(C—O_6) + 29\nu(C—O_5) + 20\delta(CO_2^-) + 10\nu(CC)$
ν_{21}	1207	1227	68.99	$25\delta(CH) + 35t(CH_2) + 12r(NH_2)$
ν_{22}	1160	1151	38.86	$40\delta(CH) + 30r(NH_3^+)$
ν_{23}	1124	1120	1.94	$35r(NH_2) + 17\nu(C—NH_2) + 15\delta(CO_2^-)$
ν_{24}	1103		69.71	$71r(NH_3^+) + 30\delta(CH) + 16\delta(skel)$
ν_{25}	1001	983	9.29	$35r(CH_2) + 27\nu(C—NH_3^+) + 26\nu(CC)$
ν_{26}	972	926	21.38	$46r(CH_2) + 40\nu(CC)$
ν_{27}	885	864	56.88	$79\delta(skel) + 17\nu(CC) + 15r(NH_3^+) + 12\gamma(NCO)$
ν_{28}	822	827	28.42	$48\nu(C—NH_3^+) + 30\nu(CC) + 15\delta(CO_2^-) + 16r(CH_2)$
ν_{29}	790	800	192.73	$30\delta(CO_2^-) + 23\nu(CC) + 26\gamma(NCO) + 15\delta(skel)$
ν_{30}	762	765	28.24	$37\nu(CC) + 25\gamma(OCO^-) + 11\delta(skel)$
ν_{31}	750		80.82	$24\delta(CO_2^-) + 22\nu(CC) + 15\gamma(NCO) + 13\nu(C—NH_3^+)$
ν_{32}	630	605	231.11	$32\gamma(NH_2) + 29\tau(NH_2)$
ν_{33}	576		182.50	$26\tau(NH_2) + 20\nu(CC) + 15\gamma(NH_2) + 12\delta(skel)$
ν_{34}	556	520	189.76	$35\gamma(NH_2)24\tau(NH_2) + 14\delta(CO_2^-) + 13\nu(CC)$
ν_{35}	522		35.23	$56\delta(CONH_2) + 16\tau(NH_2) + 12\nu(CC)$
ν_{36}	501		68.18	$45\delta(CO_2^-) + 17\nu(CC) + 15\delta(skel)$
ν_{37}	450		12.09	$54\delta(skel) + 40\delta(CONH_2) + 27\tau(skel) + 20\tau(NH_3^+)$
ν_{38}	440		10.60	$83\tau(NH_3^+) + 14\delta(skel) + 12\delta_a(NH_3^+)$
ν_{39}	409		8.72	$89\delta(skel) + 37\delta(CONH_2) + 21\tau(skel) + 11\gamma(OCO^-)$
ν_{40}	329		87.16	$67\delta(skel) + 27\delta(CO_2^-) + 15\tau(NH_3^+) + 14\nu(N—H_{10})$
ν_{41}	267		48.71	$64\delta(skel) + 14\delta(CO_2^-)$
ν_{42}	209		20.32	$46\delta(skel) + 17\tau(CO_2)) + 13\delta(CONH_2)$
ν_{43}	130		80.52	$91\tau(skel) + 27\gamma(NH_2)$
ν_{44}	101		8.85	$123\tau(CO_2^-) + 19\tau(skel)$
ν_{45}	44		51.47	$125\tau(skel) + 45\tau(CO_2^-) + 44\tau(NH_3^+)$

[a] Scaled by 0.9
[b] Arbitrary numbering
[c] See Table 6 for coordinate descriptions. Contributions from coordinates with the same character have been added to clarify the normal mode descriptions

decrease on going from 3-21G* to 6-31+G*/SCRF, namely N_8—H_{10} and C_1—C_2; both of them are involved in the five-membered ring built between the ammonium and carboxylate moieties, so that their shifts agree with the increase in the O_6—H_{10} distance. We would expect a similar behaviour for the C_1—O_6 bond, but the solvation of the carboxylate group causes minor lengthening of this bond. As a consequence, its optimized bond lengths are very close in gas phase and solution for the two ab initio basis sets. This is not the case for the C=O bond, the length on which increases by 0.003 Å when changing from vacuum to solution when the 6-31+G* is used. The polar medium also enhances the charge separation degree, giving rise to an increase of the O_{14} atomic charge by 0.026 e (see Table 5). We would like to emphasize the good agreement between these data and those reported by Wong et al. [27] for the oxygen atom of formaldehyde in acetonitrile solution ($\varepsilon = 35.9$), 0.005 Å and 0.026 e, respectively, from a HF/6-31+G*/SCRF study. The interatomic contacts discussed above also give rise to a relatively small C_2—N_8—H_{10} angle in the two 3-21G* optimized structures, 97.30 and 99.92 deg. for the isolated and solvated molecule, respectively. Also in this case the 6-31+G*/SCRF value is closest to the experimental one. As happened with other bond lengths and angles, the optimized values for the C_2—N_8—H_{10} bond angle correlate well with the $H_{10}\cdots O_6$ interatomic distance. Finally, the dihedral angles agree with the general trend observed for bond lengths and angles, with the 6-31+G*/SCRF structure fitting best the experimental values obtained for monohydrated asparagine.

Table 9. 6-31+G*/gas phase and experimental frequencies[a] (cm^{-1}) and infrared intensities ($km \cdot mol^{-1}$) calculated for asparagine

Vibration[b]	Calc.	Exp.[c]	IR int.	P.E.D. (greater than 10%)[d]
ν_1	3523		81.10	$100\nu_a(NH_2)$
ν_2	3414		74.82	$100\nu_s(NH_2)$
ν_3	3397		88.48	$96\nu(N—H_{11})$
ν_4	3288		231.44	$94\nu(N—H_9)$
ν_5	3074		218.45	$94\nu(N—H_{10})$
ν_6	3000	2965	1.80	$75\nu_a(CH_2) + 24\nu_s(CH_2)$
ν_7	2955	2945	13.85	$99\nu(CH)$
ν_8	2913	2907	16.37	$76\nu_s(CH_2) + 25\nu_a(CH_2)$
ν_9	1738		797.80	$59\nu(C—O_5) + 42\nu(C—O_6)$
ν_{10}	1706		218.44	$67\nu(C=O) + 13\nu(C—NH_2) + 10\delta(NH_2)$
ν_{11}	1662		44.32	$93\delta_a(NH_3^+)$
ν_{12}	1629	1611	80.21	$83\delta(NH_2) + 10\nu(C=O)$
ν_{13}	1606	1538	43.00	$78\delta_a(NH_3^+)$
ν_{14}	1468		37.33	$86\delta(CH_2)$
ν_{15}	1447	1450	361.94	$83\delta_s(NH_3^+)$
ν_{16}	1408	1421	158.12	$23\delta(CH_2) + 23\nu(C—NH_2) + 15\nu(CC) + 14\omega(CH_2)$
ν_{17}	1369	1404	165.31	$25\nu(C—O_6) + 23\delta(CH) + 14\nu(CC) + 12\omega(CH_2)$
ν_{18}	1346	1356	78.31	$58\delta(CH)$
ν_{19}	1311	1329	54.79	$43\omega(CH_2) + 13\nu(C—O_6) + 13\nu(C—NH_2) + 10\nu(C—O_5)$
ν_{20}	1290	1314	52.35	$33\omega(CH_2) + 19\nu(CC) + 10t(CH_2) + 10r(NH_3^+)$
ν_{21}	1202	1227	35.32	$54t(CH_2) + 15\delta(CH)$
ν_{22}	1133	1151	7.83	$36r(NH_2) + 11r(NH_3^+) + 11\nu(C=O) + 10\delta(CH)$
ν_{23}	1095	1120	22.39	$29r(NH_3^+) + 20\delta(CH) + 11r(NH_2) + 10t(CH_2)$
ν_{24}	1082		11.88	$58r(NH_3^+) + 20\delta(CH) + 19\delta(skel)$
ν_{25}	1006	983	4.16	$20\nu(CC) + 26r(CH_2) + 24\nu(C—NH_3^+)$
ν_{26}	957	926	31.46	$30r(CH_2) + 30\nu(CC) + 30r(NH_3^+)$
ν_{27}	893	864	21.54	$45\delta(skel) + 21\nu(CC) + 18r(NH_3^+) + 11\gamma(NCO)$
ν_{28}	849	827	49.19	$35\nu(CC) + 25\nu(C—NH_3^+) + 24\delta(CO_2^-) + 23r(CH_2)$
ν_{29}	797	800	55.49	$24\delta(CO_2^-) + 21\nu(C—NH_3^+) + 19\nu(CC) + 18\gamma(NCO)$
ν_{30}	781	765	38.03	$26\gamma(OCO^-) + 25\nu(CC) + 10\delta(CO_2^-)$
ν_{31}	744		15.86	$32\gamma(NCO) + 15\delta(CO_2^-) + 12\nu(CC) + 10\gamma(OCO^-)$
ν_{32}	598	605	87.73	$42\tau(NH_2) + 19\gamma(NH_2)$
ν_{33}	566		3.74	$24\nu(CC) + 23\delta(CONH_2) + 18\delta(skel) + 17\gamma(OCO^-)$
ν_{34}	527		50.68	$38\delta(CONH_2) + 21\nu(CC) + 10r(CH_2)$
ν_{35}	515	520	240.14	$85\gamma(NH_2) + 29\tau(NH_2) + 11\nu(C—NH)_2$
ν_{36}	503		44.94	$50\delta(CO_2^-) + 13\delta(skel)$
ν_{37}	440		0.95	$57\tau(skel) + 35\delta(CONH_2) + 13r(CH_2)$
ν_{38}	396		11.39	$44\delta(CONH_2) + 70\delta(skel) + 17\tau(skel)$
ν_{39}	339		35.38	$61\delta(skel) + 14\delta(CO_2^-)$
ν_{40}	286		9.12	$105\tau(NH_3^+)$
ν_{41}	261		22.14	$45\delta(skel) + 13\delta(CO_2^-)$
ν_{42}	202		27.36	$40\delta(skel) + 27\tau(skel)$
ν_{43}	95		28.65	$85\tau(skel) + 50\delta(skel)$
ν_{44}	82		16.79	$102\tau(CO_2^-) + 36\tau(skel) + 23\tau(NH_3^+)$
ν_{45}	49		16.37	$72\tau(skel) + 34\tau(CO_2^-) + 23\tau(NH_3^+)$

[a] Scaled by 0.9
[b] Arbitrary numbering
[c] See Table 6 for coordinate descriptions. Contributions from coordinates with the same character have been added to clarify the normal mode descriptions

Table 10. 6–31+G*/SCRF and experimental frequencies[a] (cm^{-1}) and infrared intensities ($km \cdot mol^{-1}$) calculated for asparagine

Vibration[b]	Calc.	Exp.[c]	IR int.	P.E.D. (greater than 10%)[d]
ν_1	3515		148.13	$100\nu_a(NH_2)$
ν_2	3410		204.92	$100\nu_s(NH_2)$
ν_3	3361		220.75	$56\nu(N{-}H_{11}) + 45\nu(N{-}H_10)$
ν_4	3315		280.25	$44\nu(N{-}H_{10}) + 31\nu(N{-}H_{11}) + 25\nu(N{-}H_9)$
ν_5	3227		143.59	$75\nu(N{-}H_9) + 14\nu(N{-}H_{11}) + 11\nu(N{-}H_{10})$
ν_6	2966	2965	0.93	$87\nu_a(CH_2) + 13\nu_s(CH_2)$
ν_7	2939	2945	13.12	$96\nu(CH)$
ν_8	2911	2907	9.44	$84\nu_s(CH_2) + 13\nu_a(CH_2)$
ν_9	1692		237.79	$52\nu(C{=}O) + 20\delta_a(NH_3^+) + 12\nu(C{-}NH_2)$
ν_{10}	1665		661.00	$64\delta_a(NH_3^+) + 19\nu((C{=}O)$
ν_{11}	1654		762.21	$55\nu(C{-}O_5) + 37\nu(C{-}O_6)17\delta_a(NH_3^+)$
ν_{12}	1625	1611	122.01	$83\delta(NH_2) + 10\nu(C{=}O)$
ν_{13}	1589	1538	114.34	$82\delta_a(NH_3^+)$
ν_{14}	1474		496.10	$91\delta_s(NH_3^+)$
ν_{15}	1443	1450	60.97	$73\delta(CH_2) + 13\nu(CO_2^-) + 12\omega(CH_2)$
ν_{16}	1429	1421	227.37	$33\delta(CH_2) + 28\omega(CH_2) + 12\nu(CO_2^-) + 12\nu(C{-}NH_2)$
ν_{17}	1391	1404	157.25	$25\nu(C{-}O_6) + 22\delta(CH) + 20\nu(CC) + 11\nu(C{-}O_5)$
ν_{18}	1357	1356	65.31	$70\delta(CH)$
ν_{19}	1313	1329	211.84	$40\delta(CH) + 21\nu(C{-}O_6) + 10\nu(C{-}O_5)$
ν_{20}	1299	1314	225.38	$40\omega(CH_2) + 31\nu(C{-}NH_2)$
ν_{21}	1228	1227	71.73	$66t(CH_2) + 19\delta(CH)$
ν_{22}	1121	1151	49.52	$34r(NH_3^+) + 20\delta(CH)$
ν_{23}	1100	1120	21.44	$45r(NH_2) + 11\nu(C{=}O) + 10r(NH_3^+)$
ν_{24}	1074		50.18	$30r(NH_3^+) + 16\nu(C{-}NH_3^+) + 12\delta(skel) + 11r(NH_2)$
ν_{25}	1021	983	28.27	$21r(NH_3^+) + 20\nu(CC) + 13r(CH_2) + 12\nu(C{-}NH_3^+)$
ν_{26}	949	926	42.62	$33r(NH_3^+) + 30\nu(CC) + 20r(CH_2)$
ν_{27}	878	864	24.73	$34\nu(C{-}NH_3^+) + 15\nu(CC) + 13r(CH_2) + 10r(NH_3^+)$
ν_{28}	855	827	70.65	$37\nu(CC) + 20\delta(skel) + 11\gamma(OCO^-) + 10r(NH_3^+)$
ν_{29}	785	800	17.19	$42\nu(CC) + 12\delta(CO_2^-) + 11\nu(C{-}NH_3^+) + 11\gamma(OCO^-)$
ν_{30}	779	765	76.14	$27\delta(CO_2^-) + 23\gamma(OCO^-) + 13\nu(C{-}NH_3^+)$
ν_{31}	672		24.23	$27\delta(CONH_2) + 21\delta(skel) + 10\gamma(NCO)$
ν_{32}	627	605	21.34	$35\tau(NH_2) + 20\gamma(NCO) + 10\delta(CONH_2)$
ν_{33}	557		66.61	$23\delta(CONH_2) + 14\delta(CO_2^-) + 10\gamma(OCO^-) + 10\gamma(NH_2)$
ν_{34}	525	520	361.22	$68\gamma(NH_2) + 10\gamma(NCO)$
ν_{35}	513		8.71	$26\tau(NH_2) + 18\delta(CO_2^-) + 16\gamma(NH_2) + 13\gamma(NCO)$
ν_{36}	473		118.34	$31\tau(NH_2) + 30\gamma(NCO) + 19\delta(CO_2^-) + 17r(CH_2)$
ν_{37}	452		14.59	$61\delta(skel) + 24\delta(CONH_2)$
ν_{38}	346		20.92	$43\delta(CONH_2) + 37\delta(skel)$
ν_{39}	318		80.21	$61\delta(skel) + 12\delta(CO_2^-)$
ν_{40}	249		23.21	$97\tau(NH_3^+) + 18r(NH_3^+) + 17\delta(skel)$
ν_{41}	235		53.79	$53\delta(skel) + 15\tau(skel) + 10\delta(CONH_2)$
ν_{42}	206		22.35	$62\delta(skel) + 31\tau(skel) + 18\tau(NH_3^+)$
ν_{43}	92		0.91	$104\tau(CO_2^-)$
ν_{44}	85		27.02	$93\tau(skel) + 46\delta(skel)$
ν_{45}	49		13.87	$100\tau(skel)$

[a] Scaled by 0.9
[b] Arbitrary numbering
[c] See Table 6 for coordinate descriptions. Contributions from coordinates with the same character have been added to clarify the normal mode descriptions

We have evaluated complete quadratic force fields for gas-phase and solvated asparagine at both 3-21G* and 6-31+G* ab initio levels. The force constants were transformed to the set of locally symmetrized internal coordinates listed in Table 6 and were scaled by 0.81 in order to compensate for the usual systematic errors (10% in frequencies) accepted in such calculations [27–29]. The results on frequencies, infrared intensities and potential energy distribution are summarized in Tables 7–10, where experimental frequencies measured for asparagine in aqueous solution were included from Ref. 7. Table 11 lists the scaled diagonal force constants obtained in each case.

The intramolecular interactions involving the ammonium group give rise to substantial differences in the $N{-}H_9$ and $N{-}H_{10}$ stretching vibrations, whereas the $N{-}H_{11}$ stretching vibration, ν_3, is only shifted by the polar environment. Concerning the 3-21G* basis set, the unusual frequency of 2473 cm^{-1} is obtained for the $\nu(N{-}H_{10})$ vibration. This behaviour also occurs for the 3-21G*/SCRF calculation, but it is not emphasized as much. The use of a higher basis set, like 6-31+G*, significantly improves these results, although in the gas phase calculation a low $N{-}H_9$ stretching mode, ν_5, still remains. Only for the 6-31+G*/SCRF NH_3^+ stretching frequencies, ν_3–ν_5, have the three $\nu(N{-}H)$ coordinates (Table 6) extensively mixed, as expected of a molecule surrounded by a polar solvent.

Between 1700 and 1400 cm^{-1} the normal mode descriptions shown in Tables 7–10 allow us to select some frequency shifts upon solvation that are observed for both 3-21G* and 6-31+G* ab initio basis sets: (1) car-

boxylate stretching frequency ν_9 (except in Table 10, ν_{11}) decreases by 31–46 cm^{-1}; (2) amide II frequency, ν_{12}, shows negligible changes; (3) ammonium symmetrical bending frequency increases by 38–27 cm^{-1}. Although the influence of the interatomic contacts discussed previously has to be taken into account, these trends reveal that the interaction of solvent molecules with the ionized groups, NH_3^+ and CO_2^-, is stronger that those with the amide group. The remaining frequencies calculated between 1700 and 1400 cm^{-1} exhibit unequal behaviours for both basis sets. Frequencies ν_{10}, ν_{11} and ν_{13} in Tables 7 and 8 (3-21G*) show an extensive coupling between $\delta(NH_3^+)$ and ν(C=O) that does not appear in the corresponding frequencies in Tables 9 and 10 (6-31+G*). These couplings can be explained by the optimized $O_{14}\cdots H_9$ distances, which are shorter in the 3-21G* structures than in the 6-31+G* ones. Solvent effects on frequencies below 1400 cm^{-1} are in general diffuse, with few exceptions, because the vibrational coordinates involving end polar groups of asparagine that appear in this region are strongly mixed. However, the normal mode description is appreciably different on going from 3-21G* to 6-31+G*. The pure solvent effects, maintaining the ab initio basis set, also cause modifications of the potential energy distribution, especially for frequencies below 900 cm^{-1}, which significantly change the spectral pattern. The frequencies that can be clearly compared, as regarding their descriptions, follow the aforementioned trends for the highest frequencies.

The calculated scaled vibrational frequencies can be also compared with those obtained from Raman measurements on asparagine solutions [7], which were assigned on the basis of the isotopic shifts upon deuteration. The differences established for the potential energy distributions make it difficult to correlate theoretical and observed values. Nevertheless, some points can be made. As can be observed in Tables 7–10, a significant improvement occurs for the carbon-hydrogen stretching vibrations that clearly follows the path 3-21G* $\mapsto$ 3-21G*/SCRF $\mapsto$ 6-31+G* $\mapsto$ 6-31+G*/SCRF. This behaviour is also observed for the other observed bands, indicating that the frequency prediction is more basis set dependent than environment dependent, in the same way as the structural results.

The qualitative features of the calculated infrared spectra of asparagine in both gas phase and aqueous solution can be seen in Fig. 3, which has been drawn from data given in Tables 7–10. Quantitative predictions of absolute intensities are rather difficult at the Hartree-Fock level of theory [30, 31]. Figure 2 demonstrates that, although the four spectra display substantial differences, there are more changes on going from 3-21G* to 6-31+G* than from gas phase to solution. Between 4000 and 2000 cm^{-1} the spectral patterns depend mainly on the frequency values, since the calculated intensities are quite similar. In these four cases the frequencies assigned to N—H stretching vibrations (NH_2, NH_3^+) present more intensities than those assigned to C—H (CH_2, CH) vibrations; in addition, some intensity enhancements can be observed on going from gas phase to solution for both ab initio basis sets. Below 2000 cm^{-1} the SCRF spectra are comparable to the gas-phase spectra, and the bands increase in intensities in solution. This increase is emphasized for frequencies whose normal modes involve polar groups, especially NH_3^+ and CO_2^-: ν_9, ν_{15}, ν_{20}, ν_{32}–ν_{34} for 3-21G*, and ν_9–ν_{14}, ν_{19}–ν_{20} for 6-31+G*. Note that there are some exceptions, such as ν_{44}, $\tau(CO_2^-)$ or ν_{32}–ν_{36}, $\gamma(NH_2)$ and $\tau(NH_2)$, in the 6-31+G* spectra. In the case of these NH_2 vibrations some decrease seems to be due to their different potential energy distributions in gas phase and solution; the spectra in Fig. 3 show that when all the contributions are added an enhanced intensity results in this zone.

The calculated diagonal force constants (scaled by 0.81) are listed in Table 11. Off-diagonal force constants are available on request. These data show similar trends to those observed for the calculated frequencies and, in general, the 6-31+G* diagonal force constants of asparagine are smaller in a polar environment than in a

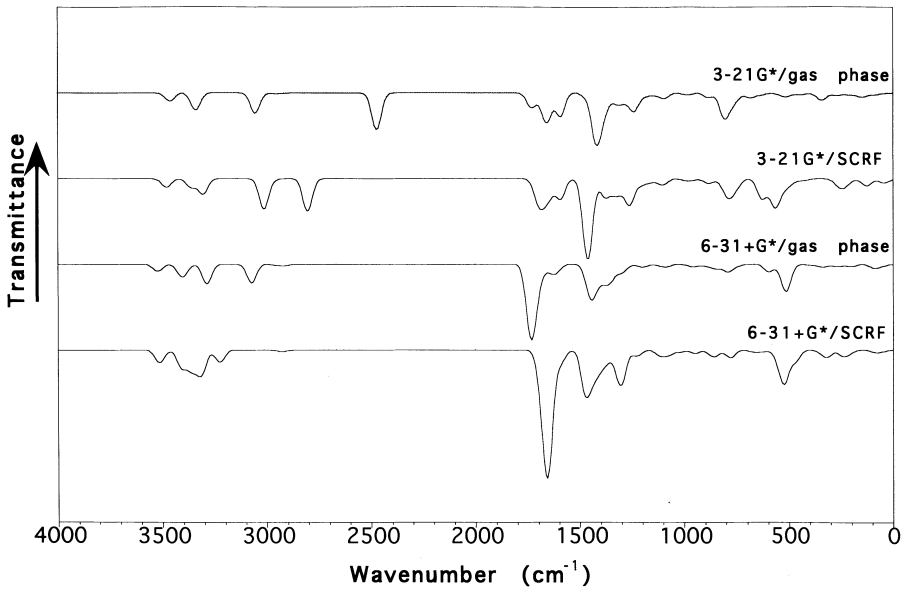

Fig. 3. Theoretical infrared spectra predicted for asparagine by ab initio methods

Table 11. Diagonal force constants[a] (in mdyn/Å) calculated for asparagine

Coordinate[b]	3-21G* gas phase	3-21G* SCRF	6-31+G* gas phase	6-31+G* SCRF
1	3.271	3.193	3.448	3.417
2	4.171	4.178	4.227	4.171
3	3.843	3.886	4.106	4.008
4	4.923	4.929	4.853	4.797
5	4.853	4.858	4.779	4.723
6	9.872	10.072	11.106	10.815
7	6.984	6.652	6.955	7.187
8	4.848	4.847	4.797	4.747
9	3.948	3.832	3.802	3.777
10	9.859	9.411	10.677	9.995
11	8.509	8.660	9.778	9.205
12	5.192	5.044	5.846	5.864
13	3.094	4.278	5.239	6.149
14	6.173	6.063	6.376	6.150
15	6.414	6.483	6.656	6.636
16	6.443	6.526	6.692	6.655
17	0.808	0.810	0.781	0.794
18	2.237	2.297	1.777	2.281
19	1.062	1.011	0.890	0.728
20	0.668	0.674	0.629	0.631
21	0.723	0.710	0.649	0.637
22	1.389	1.329	1.298	1.244
23	1.538	1.368	1.323	1.106
24	0.425	0.439	0.423	0.497
25	0.751	0.703	0.583	0.565
26	0.618	0.608	0.588	0.576
27	0.622	0.634	0.608	0.620
28	0.872	0.847	0.692	0.644
29	0.933	0.803	0.650	0.608
30	0.653	0.644	0.619	0.642
31	0.694	0.706	0.724	0.755
32	4.162	3.294	2.894	2.317
33	2.558	2.330	1.815	1.492
34	2.784	2.694	2.348	2.474
35	0.508	0.506	0.511	0.486
36	0.614	0.614	0.588	0.534
37	0.141	0.097	0.090	0.087
38	1.129	1.120	0.985	1.000
39	1.156	1.136	1.187	1.197
40	0.557	0.560	0.530	0.554
41	0.352	0.312	0.282	0.275
42	0.482	0.415	0.212	0.195
43	0.506	0.389	0.167	0.129
44	0.964	0.861	0.499	0.343
45	0.303	0.160	0.126	0.144

[a] Scaled by 0.81
[b] See Table 6 for coordinate descriptions

vacuum. Pure solvent effects can be inferred from coordinates involving atoms which are not involved in short interatomic contacts. This occurs for coordinates 10, $\nu(C{-}O_5)$ and 14, $\nu(N{-}H_{11})$, whose corresponding force constants decrease upon solvation by 6.4% and 3.5%, respectively. This difference can be explained by the fact that the atomic charge of the O_5 atom is greater, in absolute value, than the atomic charge of H_{11} atom, and that molecular steric effects permit a higher degree of solvation for the O_5 than for the H_{11} atom. Differences in force constants of other coordinates, as 6, $\nu(C{-}O)$ or 12, $\nu(N{-}H_9)$ are originated from the dual effect of the polar environment and intramolecular interactions, which cannot be easily discriminated. Diagonal force constants for the two $\nu(NH_2)$ stretching coordinates, symmetrical and antisymmetrical, show changes smaller than could be expected, but they are in agreement with their identical bond lengths calculated in a vacuum and in solution (Table 1). When the 3-21G* basis set is used, these force constants increase upon solvation. This behaviour cannot be easily explained by the Onsager theory. We would like to emphasize the large increase shown by the force constant associated with the coordinate 13, $\nu(N{-}H_{10})$, from 3.094 (gas phase/3-21G*) to 6.149 mdyn/Å (SCRF/6-31+G*), which correlates well with the calculated $N{-}H_{10}$ bond lengths. Finally, while force constants for bending coordinates in general show a similar behaviour to those for stretching coordinates, the values for torsional coordinates in the 6-31+G* scheme, 41–45, decrease upon solvation with the exception of coordinate 45, $\tau(CONH_2)$, thus indicating that intramolecular interactions, predicted at this level of ab initio calculation, are somewhat stronger than solute-solvent attractions simulated by applying a cavity model.

4 Conclusions

We have presented the results of a theoretical study of the amino acid L-asparagine in aqueous solution on the basis of the SCRF theory in combination with ab initio methodology at the RHF/3-21G* and RHF/6-31+G* levels. From this study, which has involved structural and vibrational features, the following remarks can be made:

1. The RHF/6-31+G*/SCRF force field gives a reasonable description of the vibrational behaviour of asparagine in solution. Results from the 3-21G* basis set do not allow this topic to be studied correctly. This is in good agreement with previous work, and confirms the importance of using diffuse functions to characterize polar species in solution.
2. The zwitterionic form of asparagine lies 60.30 kcal/mol lower in aqueous solution that in a vacuum. In addition, the molecular dipole moment is almost 10 D greater (7.33 and 17.21 D, respectively). As expected, solvent effects are stronger for charged moieties, NH_3^+ and CO_2^-, than for the side chain.
3. Infrared intensities are more dependent on the ab initio level (3-21G* or 6-31+G*) than on the environment (polar medium or vacuum). This conclusion could be supported by further calculations using more extended ab initio basis sets, but this not within the scope of this work. However, as has been confirmed by other authors [31], the qualitative features of the infrared spectra can be satisfactorily depicted at the RHF/6-31+G* level of theory.
4. The 6-31+G* quadratic force constants obtained in solution and gas phase indicate that intramolecular forces in asparagine are stronger than solute-solvent interactions at this level of theory.

References

1. Tse YC, Newton MD, Vishveshwara, S Pople JA (1978) J Am Chem Soc 100:4329
2. Wright LR, Borkman RF (1980) J Am Chem Soc 102:6207
3. Voogd J, Derissen JL, Van Dujineveldt FB (1981) J Am Chem Soc 103:7701
4. Bonaccorsi R, Palla P, Tomasi J (1984) J Am Chem Soc 106:1945
5. Kikuchi O, Natsui T, Kozaki T (1990) J Mol Struct (Theochem) 207:103
6. Casado J, López Navarrete JT, Ramírez FJ (1995) J Raman Spectrosc 26:1003
7. López Navarrete JT, Casado J, Hernández V, Ramírez FJ, J Raman Spectrosc (in press)
8. Casado J, López Navarrete JT, Ramírez FJ (1995) Spectrochim Acta 51A 2347
9. Wong MW, Frisch MJ, Wiberg KB, (1991) J Am Chem Soc 113:4476
10. Wong MW, Frisch MJ, Wiberg KB (1992) J Am Chem Soc 114:523
11. Wong MW, Frisch MJ, Wiberg KB (1992) J Am Chem Soc 114:1645
12. Franci MM, Pietro WJ, Hehre WJ, Binkley JS, Gordon MS, Defrees DJ, Pople JA (1982) J Chem Phys 77:3654
13. Frisch MJ, Trucks GW, Head-Gordon M, Gill PMW, Wong MW, Foresman B, Johnson BG, Schlegel HB, Robb MA, Replogle ES, Gomperts R, Andres JL, Raghavachari K, Binkley JS, Gonzalez C, Martin RL, Fox DJ, Defrees DJ, Baker J, Stewart JJP, Pople JA (1992) GAUSSIAN 92, revision C.4 Gaussian Inc., Pittsburgh, Pa
14. Biarge JA, Herranz J, Morcillo J (1961) An R Soc Esp Fis Quim Ser A 57 81
15. Pulay P, Fogarasi G, Pang F, Boggs JE (1979) J Am Chem Soc 101:2550
16. Wilson EB (1939) J Chem Phys 7:1047
17. Hickling SJ, Wooleey RG (1990) Chem Phys Lett 166:43
18. No KT, Cho KH, Kwon OY, Jhon MS, Sheraga HA (1994) J Phys Chem 98:10742
19. Onsager LJ (1936) J Am Chem Soc 58:1486
20. Chipot C, Maigret B, Rivail JL, Sheraga HA (1992) J Phys Chem 96:10267
21. Chipot C, Angyán JC, Rivail JL, Sheraga HA (1993) J Phys Chem 97:9797
22. Wang JL, Berkovitch-Yellin Z, Leiserowitz L, Acta Crystallogr. B4 (1985) 341
23. Hamilton WC (1968) In:Rich A, Davidson N (eds) Structural chemistry and molecular biology. Freeman, San Francisco
24. Alper JS, Dothe H, Coker DF (1991) Chem Phys 153:61
25. Alper JS, Dothe H, Lowe MA (1992) Chem Phys 161:198
26. Qian W, Krimm S (1994) J Phys Chem 98:9992
27. Pople JA, Krishnan R, Schlegel HB, DeFrees DJ, Binkey JS, Frisch MJ, Whiteside RF, Hout RF, Hehre WJ (1981) Int J Quantum Chem Symp 15:269
28. Fogarasi G, Pulay P (1984) Annu Rev Phys Chem 35:191
29. Bauschlinger CW Jr, Langhoff SR (1991) Chem Rev 91:701
30. Yamaguchi Y, Frisch M, Gaw J, Schaefer HF III, Binkley JS (1986) J Chem Phys 84:2262
31. Wiberg KB (1990) J Mol Struct 244:61